Janusz Pikuła, Kamil Kubik, Piotr Sędek, Marek St. Węglowski, Krzysztof Kwieciński, Robert Czech, Marcin Spólnik

Numerical Analysis in the Welding of Structures with Respect to the Minimisation of Welding Distortions

Abstract: The welding process is the subject of worldwide tests, primarily related to the effect of process conditions and parameters on the structure, geometry and the strength of joints as well as on the formation of welding stresses and strains (distortions). In spite of numerous test results, the welding process itself continues to be one of the reasons for the formation of distortions. Designers and manufacturers should follow principles contained in related standards and guidelines, specifying, among other things, acceptable dimensional deviations. The article presents FEM-based test results concerning the welding of a steel structure and analyses the effect of structure restraint on the formation of welding distortions.

Keywords: FEM, numerical analysis, welded structure, welding distortions, welding fixtures

DOI: 10.17729/ebis.2022.5/5

Introduction

For many years, welding has been commonly used all over the world, and yet, despite multiannual experience, practice, experimentation and attempted description, the process continues to entail the formation of unpredictable welding distortions. A significant heat input and related thermal cycles accompanying welding processes are responsible for the non-uniform distribution of temperature in elements being joined (in the weld) and changes of material volume [1]. The changes of material volume presented in Figure 1 take place in every direction, and, as a result, lead to the formation of various distortions in the structure. The intensity and the field of stresses and resultant welding distortions are triggered by numerous factors including thermomechanical properties of structural materials, the course of thermal processes, the variety of shapes and dimensions of structural elements being joined as well as technologies applied in the joining process and related activities such as the pre-weld preparation and the fastening of elements to be joined or cooling conditions. The set of the above-presented factors, expressed by various parameters can be divided into two, i.e. numerical and conceptual, groups. Numerical parameters include thermomechanical parameters of structural materials, parameters of

dr inż. Janusz Pikuła, mgr inż. Kamil Kubik, dr inż. Piotr Sędek, dr inż. Marek St. Węglowski, mgr inż. Krzysztof Kwieciński– Łukasiewicz – Instytut Spawalnictwa, Research Group for Materials Weldability and Welded Structures; Robert Czech, Marcin Spólnik – Naftoremont-Naftobudowa Sp. z o.o.

thermal processes and parameters determining physicochemical reactions taking place during metallurgical processes. In turn, conceptual parameters include shapes and dimensions of elements to be joined, the fastening (rigidity) of elements before, during and after the welding process, welding positons and other factors which affect the process of welding but which cannot be expressed in the form of specific numerical parameters. The appropriate determination of the aforesaid parameters depends, to a large extent, on technological experience [2–4].

Welding distortions

Welding distortions result from the combined effect of shrinkage triggered by the solidifying metal of the weld and shrinkage induced by plastic strains of areas adjacent to the weld (present during the welding process). Figure 1 presents examples of post-weld distorted elements.

Multidirectional shrinkage generated in the weld is responsible for distortions both along and across a given element. Shrinkage across the thickness of the weld is usually of little significance (and should be taken into account only in cases of very thick welds). Figure 1a presents welding distortions present in butt welded joints. In addition to generating transverse distortions (Δlx), the non-uniform action of transverse shrinkage (more intense in the excess weld metal area and less intense in the weld root) leads to angular distortion (Δα). Depending on the rigidity of elements being joined, longitudinal shrinkage along the y-axis could trigger bending (fz), sometimes adopting very complex forms and significantly distorting the structure. In cases of T-shaped elements with fillet joints, shrinkage can trigger similar reactions in the form of distortions. In addition to transverse distortion (Δlx), transverse shrinkage also triggers angular distortions (Δα). In turn, longitudinal shrinkage triggers the shortening of an element and, sometimes, its bending (depending on cross-sectional rigidity). In relation to the shape of a given structure, its dimensions as well as the length, thickness and the concentration of welds, welding shrinkage triggers distortions of various sizes and directions. The knowledge of welding distortions is an important "ally" when undertaking activities aimed to minimise or eliminate the formation of welding distortions.

Transverse distortions, resulting from transverse shrinkage, depend on the thickness of a given element, the type and dimensions of bevelling as well as on the method and technique of welding. Transverse shrinkage in T-joints with fillet welds is a more complex phenomenon, depending on the size of the weld and the thickness of elements (which usually vary). Longitudinal distortions result from longitudinal shrinkage. The length of longitudinal distortions depends not only on the volume and the length of the weld, but also on the proportion of the cross-sectional area of a given element to the cross-sectional area of the welds. The direction of weld shrinkage is consistent with the direction of the weld. Shrinkage force, resulting from

a)

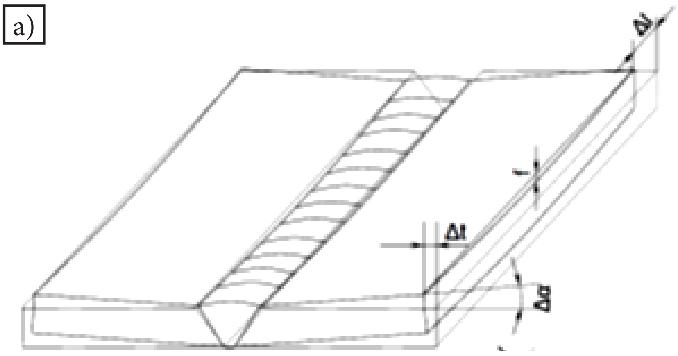

b)

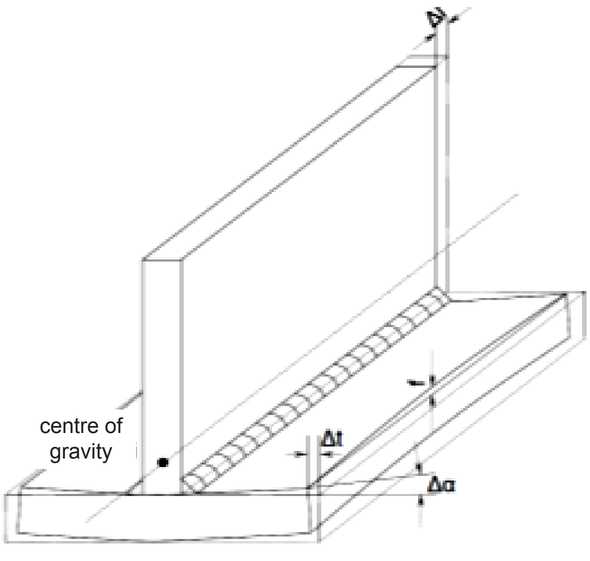

Fig. 1. Post-weld distortions in butt and T-joints

thermomechanical transformations (taking place in the weld and in the area adjacent to the weld) is distributed across the entire cross-section of the element. The plane of the aforesaid cross-section is perpendicular to the weld axis. The greater the proportion of the cross-sectional area of a given element to the cross-sectional area of the welds in a given plane, the more intense the longitudinal shrinkage.

The non-uniform transverse shrinkage of butt and fillet welds leads to angular distortions, particularly problematic as they give rise to spatial deformations including bulges, torsions, shape-related defects (flatness, linearity or perpendicularity-related deviations, etc.). Reasons for the formation of angular distortions include the non-uniform transverse shrinkage across the joint thickness and plastic deformations resulting from thermomechanical cycles. The size of transverse shrinkage depends on the angle of bevelling as well as on the width and the penetration depth of individual beads [5–8].

Forecasting of welding distortions

The forecasting of welding distortions makes it possible to optimise the welding of structures with respect to structural deformations, e.g. by using applicable welding fixtures or changing the welding sequence. Tests concerning welding distortions can involve the performance of the actual welding process or the use of finite element method-based (FEM) numerical simulations. In many industrial sectors, design processes are increasingly often supported by FEM-based tests [9–12]. Computer-aided methods enable the reduction of the number of welding tests involving test specimens. The foregoing is of particular importance (in terms of costs and laboriousness) in cases of limited possibilities of performing tests concerning the welding of actual fragments or even entire structures.

Objects of tests and model preparation

The tests concerned the welding of an element having dimensions of 4 mm × 2.4 m. The geometry of the element is presented in Figure 2a. The tests involved the definition of FEM model preparation conditions, including the application of the mesh of finite elements composed of second-order flat (2D) elements. The standard CAD geometrical model composed of bodies was used to prepare the model of the structure subjected to analysis. The model was made of internal sheet surfaces. The subsequent stage, concerned with the making of the FEM-based CAD model, involved the creation of welds.

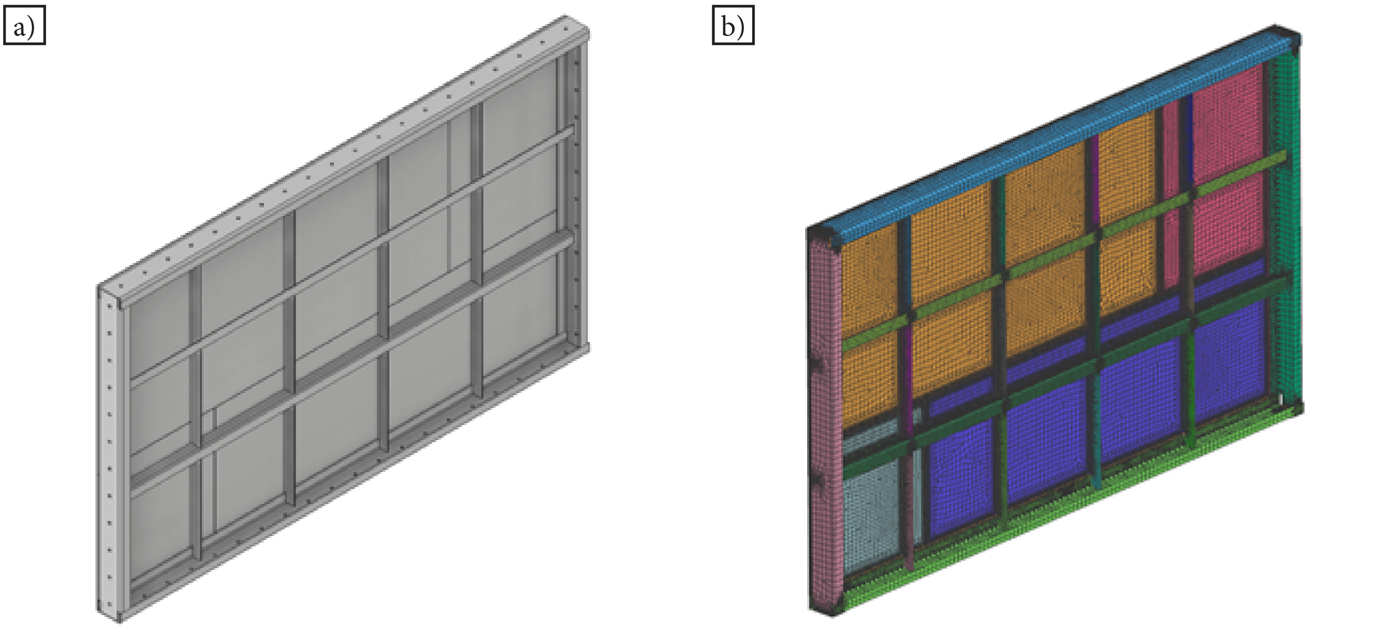

Fig. 2. Geometry (a) and the mesh of the finite elements of the model (b) of the structure subjected to analysis

Butt welds were modelled using central surfaces, whereas the width of the welds was determined on the basis of the geometry of the weld groove, defined in welding procedure specifications. Fillet welds were modelled using the weld face surface; the size of the welds was determined on the basis of weld thickness, defined in welding procedure specifications. Overlap welds were modelled using the weld face surface, whereas their size was identified on the basis of weld thickness, defined in welding procedure specifications. Skew welds (in terms of their surface) were defined as the surface perpendicular to the elements being joined; the size of the surface resulted from the distance between the elements subjected to joining. The mesh of finite elements was based on prepared surfaces (Fig. 2b). The mesh was concentrated in the crucial (i.e. joint) areas.

The modelling of the welding process involved the use of the so-called "shrinkage method". In the above-named method, shrinkage is set in the area of welded joints (Fig. 3); the value of the shrinkage is defined by the thermal expansion coefficient of a given material. The shrinkage method involves the definition of a currently made weld segment and the setting of a condition triggering shrinkage in this area. In the model, joints were divided into 53 segments. Individual elements were "provided with" material properties characteristic of steel grade S235. The width of the elements was defined in accordance with the specifications of the sheets used in the structure.

The article discusses the qualitative analysis of the effect of the manner in which a structure is fixed during welding on the geometry of the structure. The tests were concerned with the effect of various locations of clamps on welding distortions in relation to the unchanged welding sequence. The initial model (number 1) included fixing during the welding process as presented in Figure 4a. Fixing was achieved by preventing nodes located in compressed areas from moving. Alternative fixing methods involved the use of a larger number of clamps fixing the structure at points presented schematically in Figures 4b–4d.

In the models used in the tests, after the completion of the welding process, elements subjected to welding were released from the fixtures by changing the fixing-related boundary conditions presented in Figure 4 to the fixing manner presented in Figure 5. The post-weld boundary conditions were the following (Fig. 5):

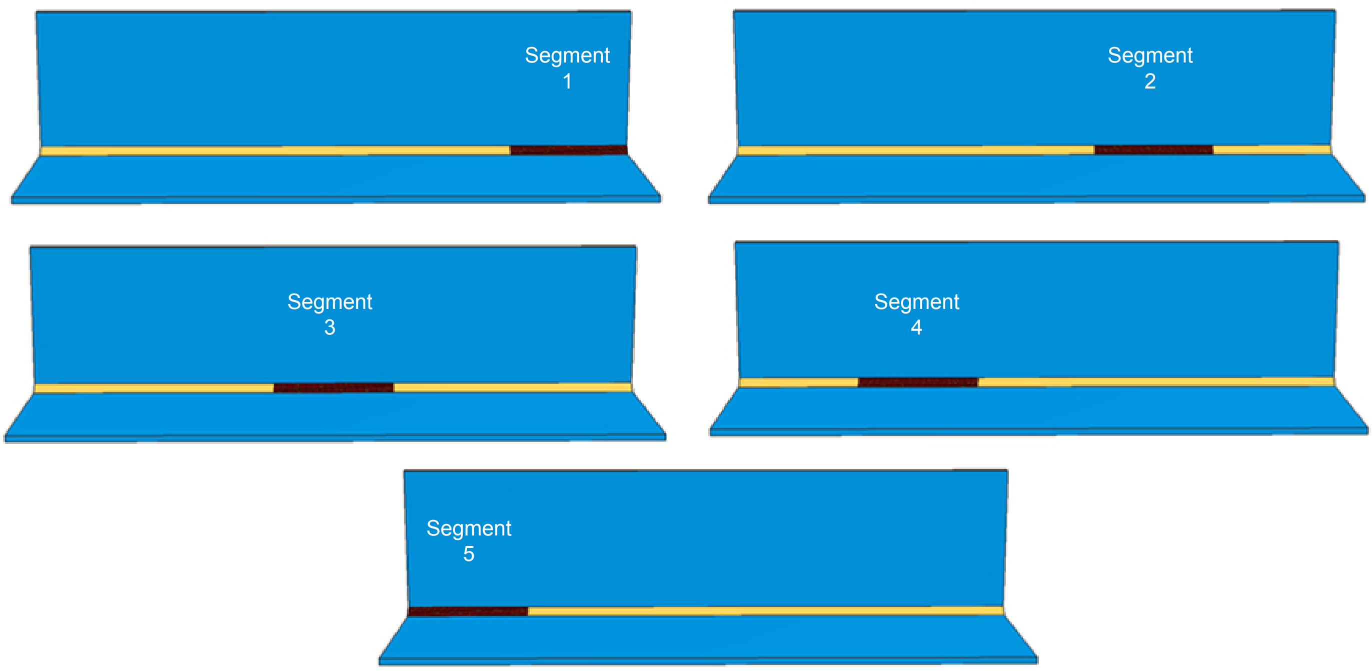

Fig. 3. "Shrinkage method"; the setting of shrinkage in successive segments of the welded joint

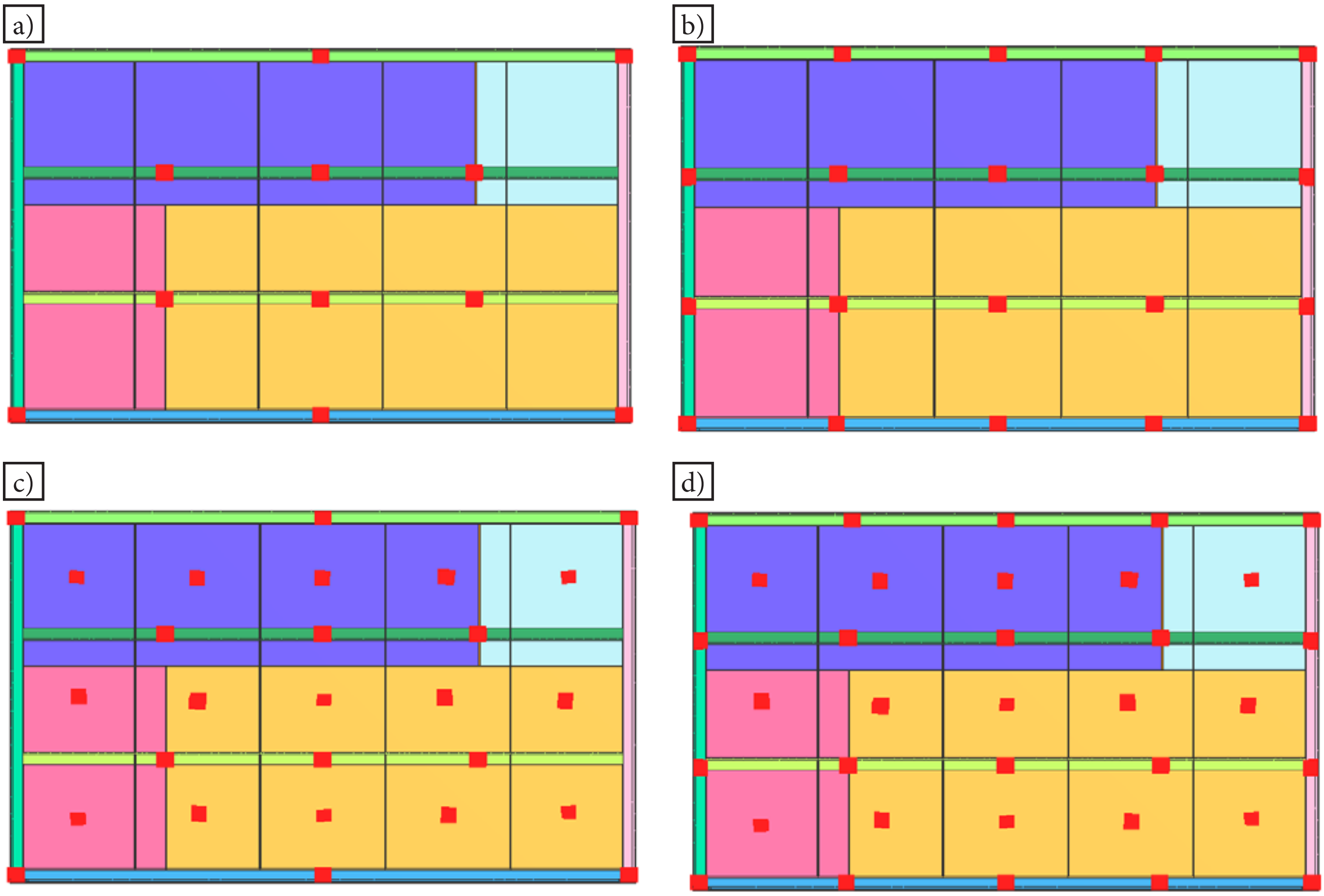

Fig. 4. Fixing arrangement (marked red): a) model 1 (initial), b) model 2, c) model 3 and d) model 4

- fixing boundary condition – impossible displacement of the node in the x, y and z-directions,
- fixing boundary condition – impossible displacement of the node in the x and y-directions,
- fixing boundary condition – impossible displacement of the node in the y-direction.

The above-presented fixing manner enabled the free distortion of the element and did not affect distortions triggered by the stiffening of the structure.

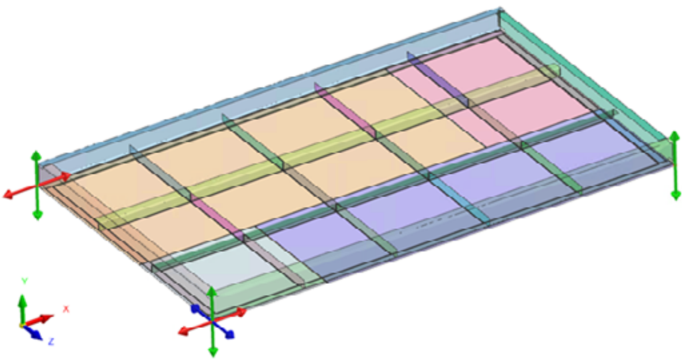

Fig. 5. Post-weld fixing conditions – impossible displacement of the nod in selected directions (x, y and z)

Test results

The field of resultant displacements is presented in Figures 6–9. After the completion of the welding process (and before releasing the specimen from the welding fixtures) the fields of displacement were characterised by significant differences, particularly noticeable in the area of the flat sheet subjected to butt welding. In turn, after the completion of the welding process and releasing the element from the welding fixtures, the field of displacements was characterised by different values of displacements, which, however, maintained similar nature. In all the models, the greatest displacements resulting from welding distortions were formed in the y-direction (perpendicular to the main surface).

The performance of the qualitative analysis of calculation results concerning displacements in the y-direction of the structure required the collection of displacement-related results at selected points. In accordance with the schematic

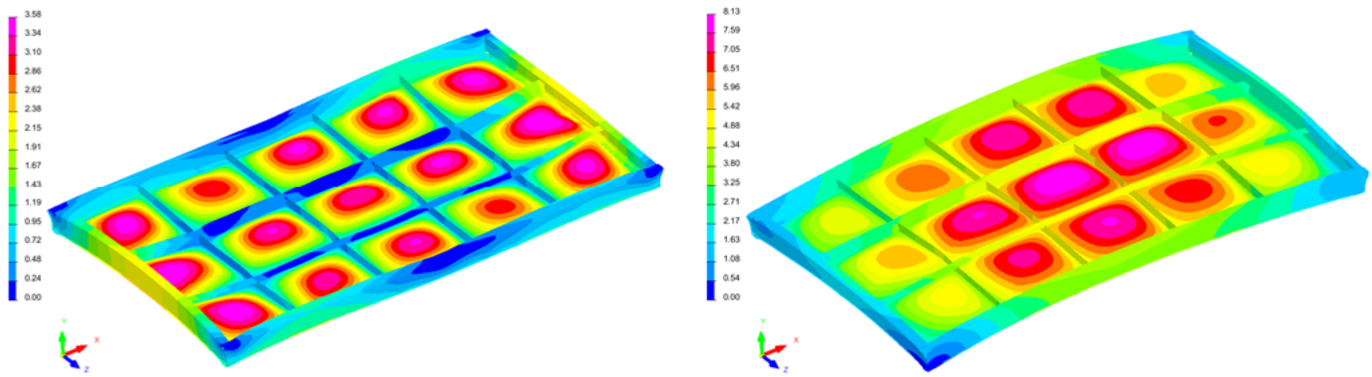

Fig. 6. Field of resultant displacements in model 1: a) after the completion of the welding process and before releasing the element from the welding fixtures and b) after the completion of the welding process and after releasing the element from the welding fixtures; element distortion scaled 40-fold, mm

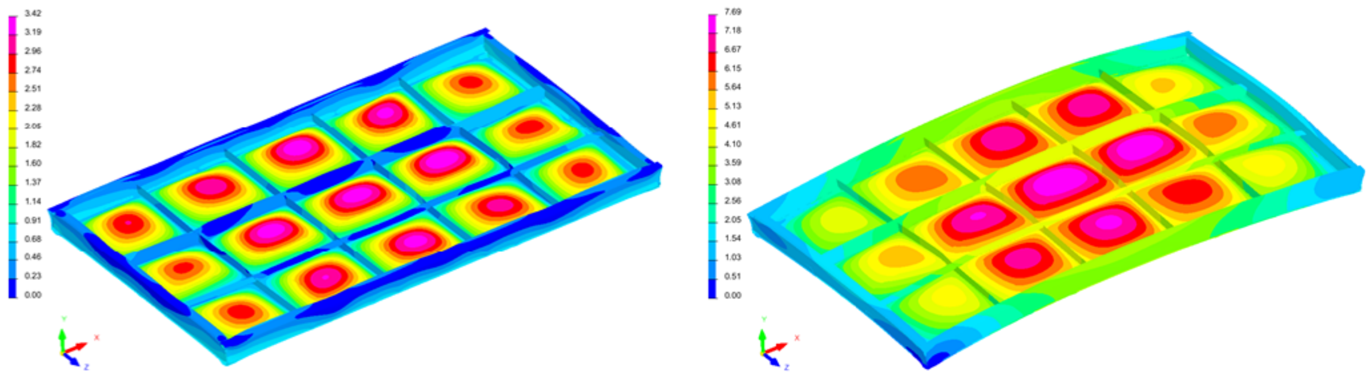

Fig. 7. Field of resultant displacements in model 2: a) after the completion of the welding process and before releasing the element from the welding fixtures and b) after the completion of the welding process and after releasing the element from the welding fixtures; element distortion scaled 40-fold, mm

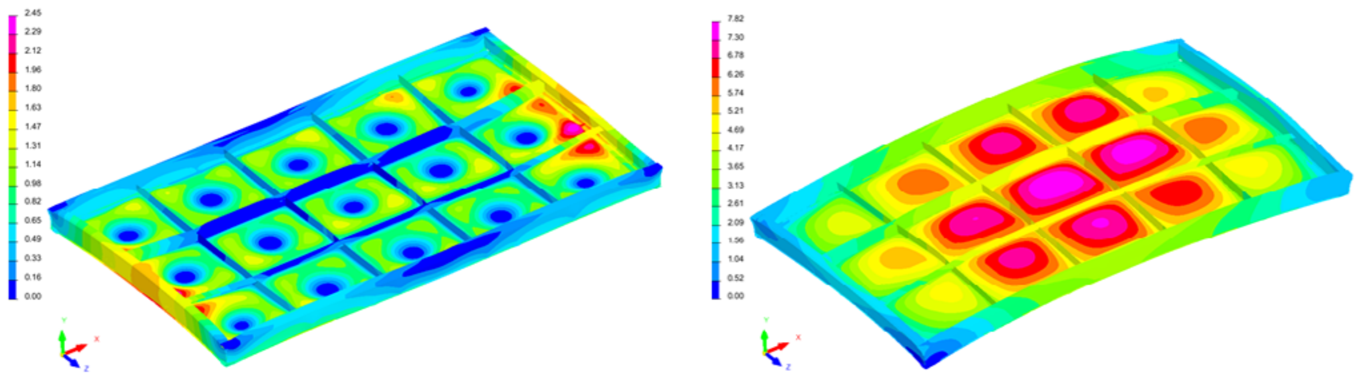

Fig. 8. Field of resultant displacements in model 3: a) after the completion of the welding process and before releasing the element from the welding fixtures and b) after the completion of the welding process and after releasing the element from the welding fixtures; element distortion scaled 40-fold, mm

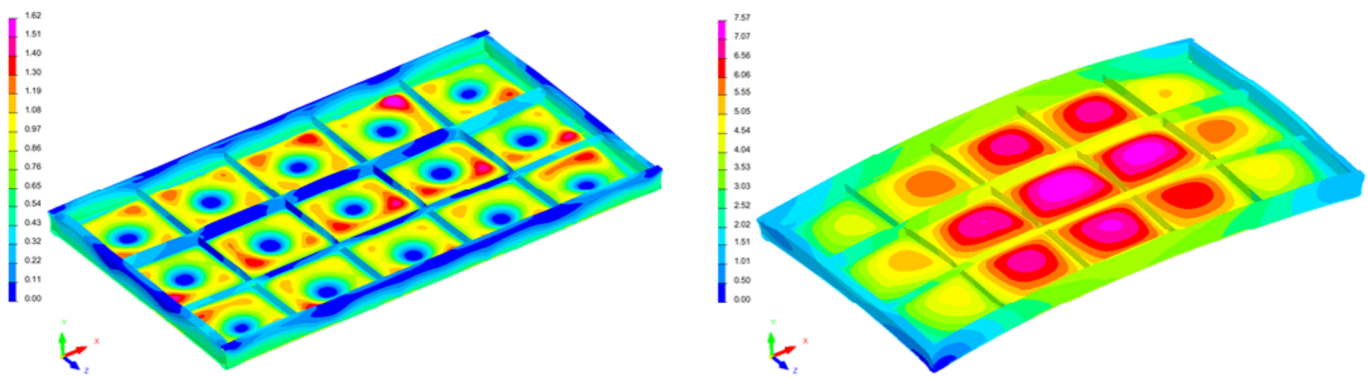

Fig. 9. Field of resultant displacements in model 4: a) after the completion of the welding process and before releasing the element from the welding fixtures and b) after the completion of the welding process and after releasing the element from the welding fixtures; element distortion scaled 40-fold, mm

diagram presented in Figure 10, the test involved the definition of 33 measurement points located on the test sheets (designated as A1-A5 as well as B1 and B2), rib sections (designated as C1-C5 and D1-D5) as well as on the channel sections of the external frame (E1-E5, F1-F5, G1-G3 and H1-H3). The results of displacements in the y-direction, at selected points, after the completion of the welding process and after releasing the structure from the clamps (change of boundary conditions to the conditions shown in Figure 5) are presented in Figures 11 and 12.

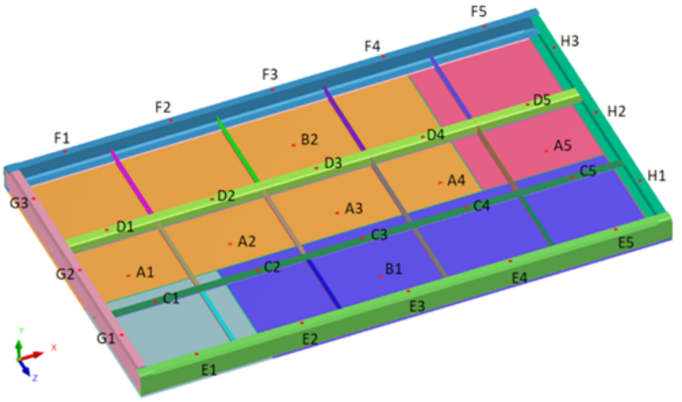

Fig. 10. Schematic arrangement of the measurement points

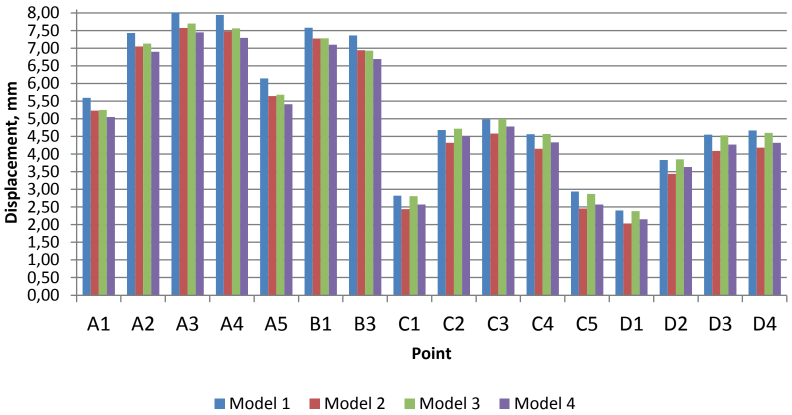

Fig. 11. Results of displacements in the y-direction at selected points (Fig. 10), after the completion of the welding process in models 1–4

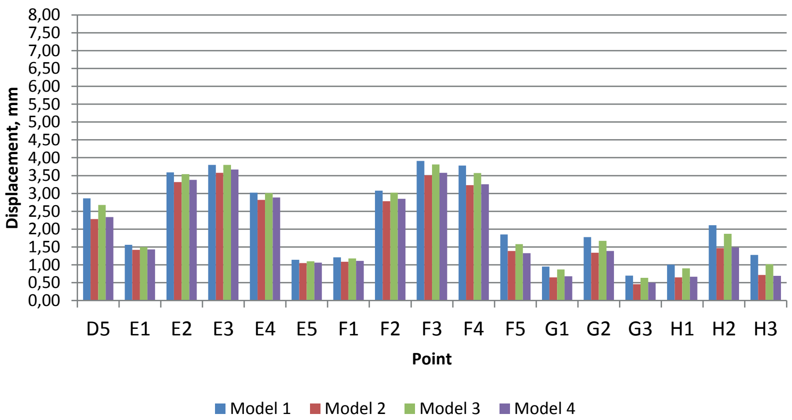

Fig. 12. Results of displacements in the y-direction at selected points (Fig. 10), after the completion of the welding process in models 1–4

The analysis of the displacements in the y-direction revealed that the stiffeners of the structure used during the welding process affected distortions during welding. In the models subjected to analysis, selected distortion-related measurement points overlapped with the stiffening points. During the welding process, the distortions at the aforesaid points adopted a value of 0 mm. At points A1, A2, A3, A4, A5, B1 and B2, at all the welding stages, greater distortions and increasing at subsequent stages of the welding process were observed in models 1 and 2. In models 3 and 4, because of stiffening applied during the welding process, the value of distortions amounted to 0 mm. At points C1, C5, D1 and D5, similar courses of displacements were observed in models 1, 2, 3 and 4. In turn, displacement values were greater in models 1 and 3. Also at points E1, E2, E5, F1, F4 and F5, the courses of displacements were similar, with the greatest values observed in model 1, and similar values observed in models 2, 3 and 4. The courses of displacements were also similar at points G1, G2, G3, H1, H2 and H3; the highest values of displacements were observed in model 1, lower values were observed in model 3, whereas the lowest and similar values were observed in models 2 and 4. The values of displacements at the other points were similar in all the models. Figure 13 presents the changes of displacements at the successive stages of the welding process in relation to point H1.

After the completion of the welding process and releasing the element from the fixing clamps (Table 1), the highest average value and the sum of displacements in the y-direction at the points subjected to analysis were observed in model 1. In comparison with model 1, smaller displacements were observed

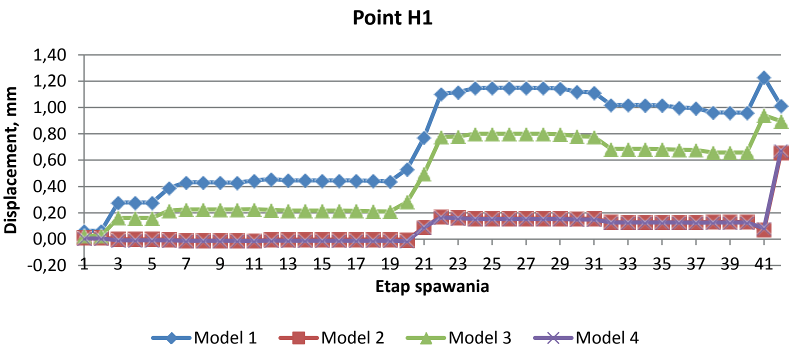

Fig. 13. Results of displacements in the y-direction at point H1 (in accordance with the schematic diagram presented in Fig. 10) at the successive stages of the welding process in models 1–4

in model 3 and, next, in models 4 and 2. The difference between the maximum average value and the sum of displacements in model 1 (largest displacements) and model 2 (smallest displacements) amounted to 11%.

Concluding remarks

The analysis of the above-presented test results justified the formulation of the following conclusions:

1. Because of their low rigidity, the spatial-flat elements were particularly susceptible to welding distortions. In cases of thin sheets of significant areas, subjected to welding involving the use of stiffeners, it was often necessary to make long welds, entailing shrinkage and leading to the corrugation of elements. After the completion of the welding process, the structure between the ribs was characterised by the presence of local bulges of the sheets. It was also possible to observe the general bulge of the whole structure.
2. In the structure subjected to analysis, dimensionally relevant displacements were present in the y-direction, perpendicular to the surface of the structure. The greatest displacements were observed in the central area of the modelled structure, in all the fixing configurations subjected to analysis.
3. The qualitative analysis of different variants concerned with the fixing of elements during the welding process revealed that the stiffening of the structure during welding enabled the reduction of welding distortions. The identified values of displacements in the y-direction at the points subjected to analysis revealed that the difference between the maximum average value in model 1 (largest displacements) and

Table 1. Test results: the average values and the sums of displacements in the y-direction at selected points (in accordance with the schematic diagram presented in Fig. 10) after the completion of the welding process in models 1–4, mm

	A1	A2	A3	A4	A5	B1	B3	C1	C2	C3	C4	C5
Model 1	5.59	7.43	8.01	7.94	6.14	7.58	7.36	2.82	4.68	4.98	4.56	2.94
Model 2	5.23	7.05	7.57	7.48	5.64	7.27	6.94	2.44	4.32	4.58	4.15	2.46
Model 3	5.25	7.13	7.70	7.56	5.68	7.28	6.93	2.81	4.72	5.00	4.57	2.87
Model 4	5.05	6.90	7.45	7.29	5.41	7.10	6.69	2.57	4.51	4.78	4.33	2.57

	D1	D2	D3	D4	D5	E1	E2	E3	E4	E5	F1	F2
Model 1	2.40	3.83	4.55	4.67	2.86	1.56	3.59	3.80	3.02	1.14	1.21	3.08
Model 2	2.03	3.44	4.09	4.18	2.28	1.42	3.32	3.58	2.82	1.05	1.09	2.78
Model 3	2.38	3.85	4.53	4.60	2.68	1.50	3.54	3.80	3.01	1.10	1.18	3.02
Model 4	2.15	3.63	4.27	4.32	2.34	1.43	3.38	3.67	2.89	1.06	1.11	2.85

	F3	F4	F5	G1	G2	G3	H1	H2	H3	**Average**	**Sum**
Model 1	3.91	3.78	1.85	0.95	1.78	0.70	1.01	2.11	1.28	3.731	123.11
Model 2	3.51	3.23	1.39	0.65	1.34	0.46	0.65	1.47	0.72	3.352	110.63
Model 3	3.81	3.57	1.58	0.87	1.67	0.64	0.90	1.87	1.02	3.595	118.62
Model 4	3.58	3.26	1.33	0.68	1.39	0.50	0.67	1.49	0.69	3.374	111.34

in model 2 (smallest displacements) amounted to 11%. The difference concerning the sum of displacements between models 1 and 2 also amounted to 11%.

References

[1] Mizerski J.: Spawanie. Wiadomości podstawowe. Wyd. REA, Warszawa 2005.

[2] Connor L.P.: Welding Handbook. Eighth Edition. Vol. 1. Welding Technology AWS 1997.

[3] Radaj D.: Heat Effects of Welding. Temperature Fields, Residual Stress Distortion. Springer-Verlag. 1992.

[4] Stewart J.P.: Distortion control. John Stewart. Canada 1996.

[5] Kelly S.M., Martukanitz R.P., Reutzel E.W.: Minimizing buckling distortion in welding by hybrid laser-arc welding – Minimization of Welding Distortion and Buckling – 9. Modelling and Implementation, Woodhead Publishing Series in Welding and Other Joining Technologies, 2011.

[6] Wang J., Yuan H., Ma N., Murakawa H.: Recent research on welding distortion prediction in thin plate fabrication by means of elastic FE computation. Marine Structures, 2016, vol. 47.

[7] Li Y., Wang K., Jin Y., Xu M., Lu H.: Prediction of welding deformation in stiffened structure by introducing thermo-mechanical interface element. Journal of Materials Processing Technology, 2015, vol. 216.

[8] Fu G., Lourenço M.I., Duan M., Estefen S.F.: Influence of the welding sequence on residual stress and distortion of fillet welded structures. Marine Structures, 2016, vol. 46.

[9] Kokot G., John A., Górka J.: Wspomaganie procesu spawania z wykorzystaniem MES. Przegląd Mechaniczny, 2008, no. 5.

[10] Kik T., Górka J.: Numerical simulations of laser and hybrid S700MC T-joint welding, Materials, 2019, vol. 12, no. 3, 516.

[11] Heinze C., Schwenk C., Rethmeier M.: The effect of tack welding on numerically calculated welding-induced distortion. Journal of Materials Processing Technology, 2012, vol. 212, no. 1.

[12] Kik. T., Slováček M.: Metody analiz numerycznych procesów spawania złożonych konstrukcji, Welding Technology Review, 2017, vol. 89, no. 5.